

# STRENGTH OF YTTRIA-STABILISED ZIRCONIA WITH NEAR-SURFACE GRINDING RESIDUAL STRESSES

A. Juy, L. Llanes and M. Anglada

Departament de Ciència dels Materials i Enginyeria Metal·lúrgica,  
ETSEIB, Universitat Politècnica de Catalunya, 08028 Barcelona

*ABSTRACT: The residual stresses induced by grinding in tetragonal zirconia polycrystals stabilised with 2.5% molar yttria (Y-TZP) have been investigated. Two Y-TZP microstructures have been analysed; one consists of very fine tetragonal grains, whereas the other exhibits a coarser duplex structure of cubic and tetragonal grains. It is shown that indentation cracks after grinding are always shorter than in the annealed condition and this effect is much larger for the coarse duplex microstructure. It is also found that biaxial flexure strength of ground specimens increases with respect to that in the annealed condition, in spite of the large number of surface defects induced by machining. These findings are analysed by Raman spectroscopy as well as by X-ray diffraction and related to changes in the near surface microstructure induced by grinding. The results are discussed within a fracture mechanics framework.*

## INTRODUCTION

Ceramic materials have excellent properties such as high hardness and resistance to oxidation, corrosion and creep at elevated temperatures. However, the characteristic low toughness of monolithic ceramic materials has hampered their wide spread utilisation. One of the most effective methods to increase fracture toughness is by transformation toughening [1]. This is particularly true in Y-TZP ceramics, whose microstructure is formed by a large volume fraction of very small metastable tetragonal grains as well as by a relatively low proportion of cubic and monoclinic grains [2]. In these materials, the exact fraction of each phase depends on the amount of oxide stabiliser, grain size, sintering temperature and time, cooling rate, etc. The source of toughening lies on the stress induced transformation of

tetragonal (t) into the monoclinic (m) zirconia polymorph that is accompanied by a volume increase of about 4%. Several factors, such as changes in free energy, particle size and strain energy, affect the transformation of the constrained tetragonal particles [2].

It is well known that by appropriate surface grinding of ceramics, microplastic deformation can occur locally in a thin surface layer, inducing residual compression stresses [3] that may increase the strength. In transformable zirconia ceramics, grinding stresses may also nucleate the t→m transformation in a surface layer, which could contribute to the increase in strength too [4]. In this paper, the effects of grinding on the strength and toughness of Y-TZP with different transformability are studied.

## EXPERIMENTAL PROCEDURE

Two zirconia ceramics stabilised with 2.5% molar of  $Y_2O_3$  were investigated: (a) a fine-grained Y-TZP, which will be referred to as AR, and (b) a Y-TZP with a mixed cubic and tetragonal microstructure, designated as 10H. The former has a very fine tetragonal microstructure, with an average grain size of 0.3  $\mu\text{m}$ ; whereas the latter consists of large tetragonal and cubic grains of mean grain sizes of 2.3  $\mu\text{m}$  and 4.6  $\mu\text{m}$ , respectively. Additional information on these materials can be found elsewhere [5].

Grinding tests were carried out in disc specimens in a laboratory automatic grinding machine with a 150 grit diamond disc and cooled with water. The applied pressures were 0.09, 0.5 and 0.9 MPa and the velocity of cut was maintained constant in all tests and equal to 3.5 m/sec. Other specimens were ground and carefully polished with diamond paste of grain sizes from 30 to 3  $\mu\text{m}$ , and finally subjected to a thermal treatment at 1200 °C during 12 minutes in order to revert any t→m transformation caused during preparation. The volume fraction of monoclinic phase was estimated by both Raman spectroscopy and X-ray diffraction (XRD).

Vickers indentations were conducted at various loads and with the maximum load applied during a period of 15 s. A drop of oil was used in order to avoid slow crack growth by the influence of humidity in air. Crack length was measured by means of an optical microscope with Nomarski interference contrast and resolution of 1  $\mu\text{m}$ .

The fracture strength was measured in biaxial flexion using a miniaturised ball-on ring testing fixture using thin discs of diameter 8 mm and thickness  $0.90\pm 0.05$  mm. The load was applied by means of a cemented carbide ball of 1.6 mm in diameter at a rate of 100 N/s and the biaxial

strength was obtained by using the expression proposed in [6]. The radius of the circle of uniform loading was taken equal to one third of the disc thickness.

## RESULTS AND DISCUSSION

The indentation crack length,  $l$ , is presented in Figures 1 and 2 in terms of the indentation load,  $P$ , for both AR and 10H, for specimens polished and heat treated to remove any surface residual stress ( $P$ ), as well as for specimens ground ( $G$ ) under a constant pressure of 0.9 MPa. Notice that for AR, in both material conditions, there is a linear relationship between  $l$  and  $P$ . By contrast, this does not hold for 10 H. Additionally, for a given load,  $l$  is always smaller in the ground specimens, and this effect is larger for 10H. This is an indication of the existence of residual compressive stresses in a surface layer.

Indentation cracks were of Palmqvist-type. Fracture toughness was obtained by using an expression proposed by Niihara et al [7]

$$K_{Ic} = C \left( \frac{E}{H_V} \right)^{\frac{2}{5}} \left( \frac{P}{dl^{1/2}} \right) \quad (1)$$

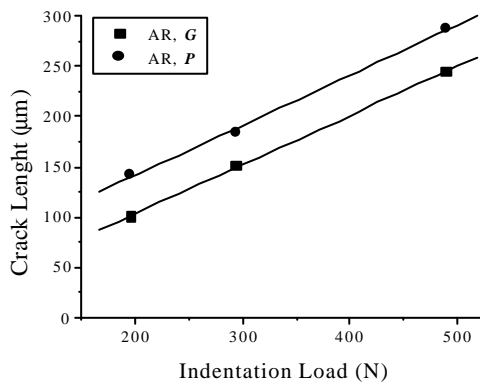


**Figure 1:** Indentation crack length versus applied load for AR.

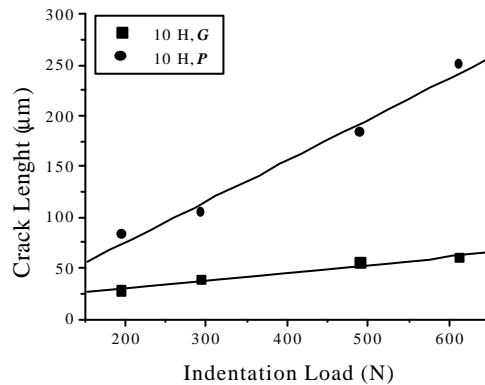


**Figure 2:** Indentation crack length versus applied load for 10H.

for  $l/d > 1$ , and where  $E$  is the elastic modulus,  $d$ , the indentation half-diagonal,  $H_v$  the Vickers hardness and  $C$  a constant. For AR the ratio  $l/d$  is larger than 1 for loads equal or higher than 100 N (Figure 1). However, for 10H the above condition does not hold for loads lower than 600 N. Then, equation (1) was only used for loads higher than this value. However, for ground specimens of 10H, indentation cracks were too small, and did not obey the above condition. The values of  $K_{Ic}$  are  $4.3 \text{ MPa m}^{1/2}$  for AR and  $8.8 \text{ MPa m}^{1/2}$  for 10H as has been reported elsewhere [8].

The strength of the surface residual stress field diminishes rapidly below the surface. By a sequence of steps of polishing and indenting the specimens, it was possible to find out the depth at which the lengths of indentation cracks recover their original value before grinding. It is in the range between 3 and 8  $\mu\text{m}$  and depends on grinding conditions.

By sectional grinding it was found that for 10H the shape of the crack is approximately semi-elliptical with a ratio  $a/l$  that changes from about 0.6 in the annealed condition to about 0.9 in the ground specimens. Hence, in the latter the indentation crack can extend much easily in the depth direction than along the surface, which is where the compressive residual stresses are larger.

The biaxial strength of both AR and 10H was measured before and after grinding and the results are plotted in the form of Weibull plots in Figures 3 and 4. It may be seen that grinding increases the biaxial strength, and this effect is larger for 10H.

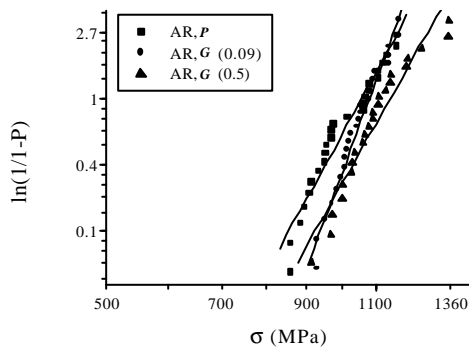


**Figure 3** : Weibull plot for AR

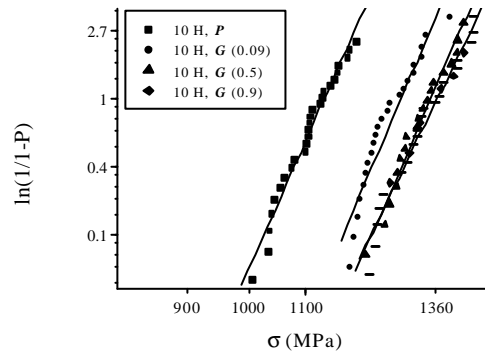


**Figure 4** : Weibull plot for 10H

Attempting to evaluate the damage induced by grinding, 10H ground specimens were heat treated at 1200 °C for 12 minutes (G+A) in order to revert any t→m transformation that could have taken place during grinding, and that may shield the surface defects from applied stresses (Figure 5). It may be noticed that the specimen ground with the highest pressure and later annealed, do not have the lowest strength. It means that in 10H the strength dominant defects do not always increase with the applied grinding pressure. The modulus of Weibull and characteristic strength for all sets of specimens are shown in Figure 6 and Table 1.

The surface of the specimens was analysed by Raman spectrometry and by XRD. By comparing the Raman spectrum of 10H in specimens polished and stress relieved (Figure 7) with that after grinding (Figure 8), it is discerned that the latter does not show the existence of a significant amount of monoclinic phase. This unexpected result was confirmed by XRD.

TABLE 1: Characteristic Weibull strength for 10H

Surface condition	P	G(0.09)	G(0.5)	G(0.9)	G+A (0.09)	G+A (0.5)	G+A (0.9)
$s_0$ (MPa)	1136	1284	1353	1372	1037	1009	1085

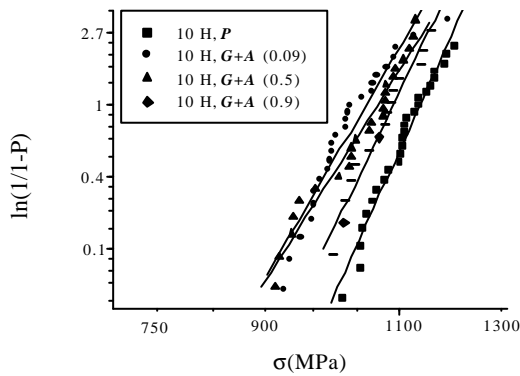


Figure 5 : Strength for polished, and ground + annealed specimens of 10 H.

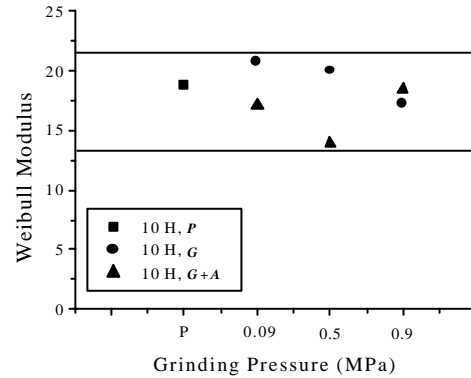


Figure 6 : Weibull modulus for 10H

In order to simplify the discussion, let us assume that failure is always originated by natural cracks and that are distributed in such a way that they produce an inert strength Weibull distribution with a strength,  $s_i$ , for a given surface condition, and Weibull parameters  $m_i$  and  $s_{0,i}$ . We also neglect R-curve effects, and assume that no crack extension takes place before failure.

The difference,  $\Delta s$ , between the inert characteristic fracture strengths of ground and stress relieved 10H specimens, may be used as a measure of the effect of grinding residual stresses. Thus,

$$\frac{\Delta s}{s_g} = \frac{K_{res}}{K_{lc}} \quad (2)$$

where  $s_g$  is the strength in the ground specimens in the absence of residual stresses; and  $K_{res}$  is the stress intensity induced by the residual stress field. The resulting value of the above ratio depends on the grinding pressure. Its highest value is 26% for 0.9 MPa. To further proceed to obtain the residual stress, it is necessary to know the functional dependence of the residual stresses with depth.

It is well known that the stress field measured by XRD in different ceramic materials after grinding diminishes very rapidly with depth [3]. One of the simplest expressions used [9] to account for this strong decay with depth,  $x$ , is simply given by:

$$s = s_0 \exp(-I x) \quad (3)$$

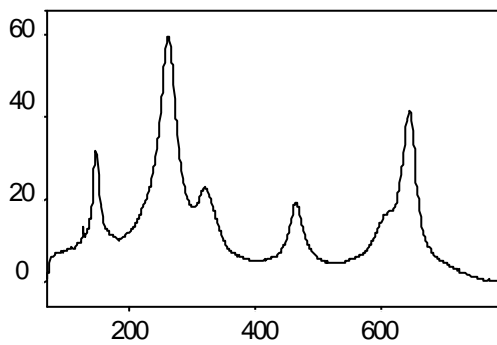


**Figure 7 :** Raman spectrum for polished and annealed 10 H material.

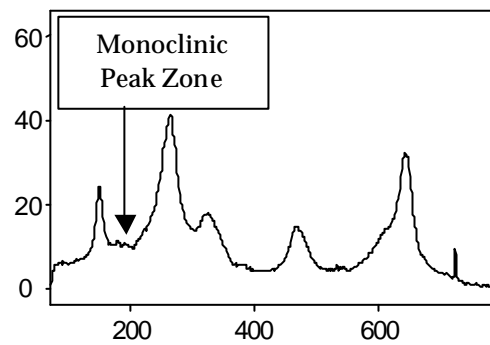


**Figure 8 :** Raman spectrum for 10H after grinding.

where  $s_0$  is the maximum strength value of the residual stress field at the surface and  $I$  is a measure of the decay of the residual stress with the distance to the surface. Assuming that surface cracks are of semi-elliptical shape, then the stress intensity factors at the deepest point, A, and for a point at the surface, B, are given by [10],

$$K_{A,B} = s_0 Y_{A,B} \sqrt{l/2} \quad (4)$$

where  $Y_{A,B}$  are functions of  $\lambda$  and  $l/2$ . Since the residual stress field exhibits a very strong gradient, i.e. it vanishes within a few micrometers, then  $I(l/2) \gg 1$ . The residual stress intensity factor has a high negative value at point B on the surface, while at point A it is much less negative so that fracture toughness shall be reached at A before that at B. Then the crack may start to propagate locally inside the specimen. This explains the marked eccentricity of indentation cracks in ground specimens mentioned above.

Now we shall additionally assume that natural defects are semicircular and that failure takes place when the total stress intensity factor at point A reaches  $K_{Ic}$ . Then by using  $K_{Ic} = s_f Y \sqrt{(l/2)}$ , where  $s_f$  is the flexural strength of the annealed specimens, the maximum residual stress field,  $s_0$ , may be estimated,

$$s_0 = s_f \frac{K_r Y}{K_{Ic} Y_A} \quad (5)$$

$Y/Y_A$  is the ratio between the geometric function for  $K$  for a surface semicircular crack in bending and that for  $K$  for the residual stress profile.  $Y$  is given by 1.16 whereas  $Y_A$  is estimated to be 0.99, considering  $I \approx 0.25 (\mu\text{m})^{-1}$ . As a result, the maximum stress field originated is about 40 % of the strength.

This result is consistent with the observation that no significant amount of monoclinic phase is found at the surface of the ground specimens by Raman spectroscopy and by XRD. Then, the source of residual stresses is not directly related to irreversible t→m transformation, and it is consistent with the maximum residual stress level reached at the surface, which is lower than the transformation critical stress.

## CONCLUSIONS

Grinding decreases the length of indentation cracks and increase the biaxial strength of Y-TZP with a coarse duplex microstructure of cubic and tetragonal grains. Both effects are much smaller in Y-TZP with a fine complete tetragonal microstructure. The residual stresses that are responsible for these changes are not related to the t→m transformation, since the monoclinic phase is nearly absent at the surface of ground specimens of the duplex coarse Y-TZP microstructure.

## ACKNOWLEDGEMENTS

The authors gratefully acknowledge the Spanish Comisión Interministerial de Ciencia y Tecnología for its financial support under grant No. MAT-99-0781 and Mat-200-1014-C02-01 to the Generalitat de Catalunya under grant No.1999SGR00129.

## REFERENCES

1. Evans, A. G. (1992) *J. Am. Ceram. Soc.* **73**, 187.
2. Hannink, R.H.J., Kelly, P.M. and Muddle, B. C. (2000) *J. Am. Ceram. Soc.*, **83**, 461.
3. Pfeiffer, W and Rombach, W. and Sommer, E. (1996). In: *Fracture Mechanics of Ceramics*, **11**, 401, Hasselman, D.P.H., Munz, D., Sakai, M. and Shevchenko (Eds.). Plenum Press, New York.
4. Swain, M.V. and Hannink, R.H.J. (1989) *J. Am. Ceram. Soc.* **72**, 1358.
5. Casellas D., Llanes L., Cumbreira F., Sánchez-Bajo F., Forsling W. and Anglada M. (2001) *J. Eur. Ceram. Soc.*, **21**, 147.
6. De With, G. and Wagemans, H.H.M. (1989) *J. Am. Ceram. Soc.*, **72**, 1538.
7. Niihara, K., Morena, R. and Hasselman D.P.H (1982) *J. Mater. Sci. Lett.* **13**, 6.
8. Casellas, D., Alcalá, J., Llanes, L. and Anglada, M. (2001) *J. Mater. Sci.* **36**, 301.
9. Fett, T. and Munz, D. (2002) In: *Fracture Mechanics of Ceramics*, Plenum Press, New York, in press.
10. Fett, T., Munz, D. (1999) *Engng. Fract. Mech.*, **64**, 105.